Science Bulletin 64 (2019) 625–633

Contents lists available at ScienceDirect

Science Bulletin

journal homepage: www.elsevier.com/locate/scib

Article

An efficient and innovative catalytic reactor for VOCs emission control

Achraf El Kasmi [a], Guan-Fu Pan [a,b,1], Ling-Nan Wu [a], Zhen-Yu Tian [a,b,*]

[a] Institute of Engineering Thermophysics, Chinese Academy of Sciences, Beijing 100190, China
[b] University of Chinese Academy of Sciences, Beijing 100049, China

ARTICLE INFO

Article history:
Received 26 January 2019
Received in revised form 4 March 2019
Accepted 28 March 2019
Available online 3 April 2019

Keywords:
Novel catalytic jet-stirred reactor
Heterogeneous kinetic study
Exhaust emission control
CuO thin film catalyst
DFT calculation

ABSTRACT

Efficient mixing and thermal control are important in the flow reactor for obtaining a high product yield and selectivity. Here, we report a heterogeneous chemical kinetic study of propene oxidation within a newly designed catalytic jet-stirred reactor (CJSR). To better understand the interplay between the catalytic performances and properties, the CuO thin films have been characterized and the adsorbed energies of propene on the adsorbed and lattice oxygen were calculated using density functional theory (DFT) method. Structure and morphology analyses revealed a monoclinic structure with nano-crystallite size and porous microstructure, which is responsible for holding an important quantity of adsorbed oxygen. The residence time inside the flow CJSR (1.12–7.84 s) makes it suitable for kinetic study and gives guidance for scale-up. The kinetic study revealed that using CJSR the reaction rate increases with O_2 concentration that is commonly not achievable for catalytic flow tube reactor, whereas the reaction rate tends to increase slightly above 30% of O_2 due to the catalyst surface saturation. Moreover, DFT calculations demonstrated that adsorbed oxygen is the most involved oxygen, and it has found that the pathway of producing propene oxide makes the reaction of C_3H_6 over CuO surface more likely to proceed. Accordingly, these findings revealed that CJSR combined with theoretical calculation is suitable for kinetic study, which can pave the way to investigate the kinetic study of other exhaust gases.

1. Introduction

Exhaust emissions containing volatile organic compounds (VOCs) are recognized as the main pollutants issued from industrial processes, fossil fuel combustion, transportation, etc.; due to their high toxicity and harmful effects on the human health and air quality [1–5]. It is therefore urgent to develop appropriate and efficient technologies to reduce VOC emissions in the context of a clean approach. Catalytic oxidation technology is one of the promising technologies for the abatement of exhaust gases [6,7], especially for short-chain unsaturated hydrocarbons such as propene (C_3H_6) [8,9]. Low-temperature of C_3H_6 catalytic oxidation is of great importance owing to the consideration of low cost, energy saving, safety and environmental friendliness [10]. In this regard, catalytic oxidation for C_3H_6 removal has been studied using catalytic flow reactors [10–12]. However, the catalytic kinetic study is quite limited, especially the achievement of highly efficient oxidation depends greatly on the reactor design. Thanks to the long residence time and high homogeneity of the gas phase within spherical Jet-Stirred Reactor (JSR) [13], the homogeneous gas-phase kinetic study on JSR has been widely performed. However, JSR has been scarcely applied to catalytic studies. It is thus desirable to develop catalytic JSR (CJSR), which could provide a long residence time for such purposes.

Catalytic oxidation of C_3H_6 has been reported previously using precious metals owing to their high activity at low temperature [10,12,14,15]. However, because of the high price, the tendency to the poison and limited resources of such noble metals, high interest was given to develop transition metal oxide catalysts, regarding their highly thermal stability, low cost, and competitive performance at low temperature [16–18]. Furthermore, the facility and high reproducibility to synthesize very active catalysts makes single oxides as attractive catalysts [19]. Among them, CuO is abundantly available, non-toxic and has been exploited in various applications [20,21]. However, the application of CuO catalyst for the abatement of exhaust gases is not much known [22]. Moreover, the use of materials based thin films is also of high importance to import properties that are different from that of the bulk material or can be otherwise unattainable by bulk material, which had attracted much interest in the last decade [23]. Hence, considering the use of film catalyst will reduce the amount of the used material and as a consequence can significantly reduce the catalyst's price

* Corresponding author.
E-mail address: tianzhenyu@iet.cn (Z.-Y. Tian).
[1] Present address: Energy Conservation Corporation Ltd. of China Coal Research Institute, Beijing 100013, China.

https://doi.org/10.1016/j.scib.2019.04.001
2095-9273/

and render it more competitive in the market. Compared to the above-mentioned techniques, pulsed-spray evaporation chemical vapor deposition (PSE-CVD) is an inexpensive and easy technique for the synthesis of continuous film oxides with high purity on numerous kinds of substrates without any after-treatment. Recently, it has been successfully performed to synthesize a series of active catalysts based transition metal oxides for low-temperature catalytic oxidation [11,24–26]. It is therefore important to synthesize film catalysts with PSE-CVD technique for catalytic kinetic study of C_3H_6 using CJSR.

The present study aims to investigate CJSR as a newly-designed reactor for the kinetic study of the catalytic oxidation of C_3H_6. The attention was also paid to the preparation of CuO thin film catalysts using PSE-CVD method. The correlation of the catalytic activity with catalyst properties was addressed with respect to kinetic study, activation energy, and new reactor design. In addition, DFT theoretical calculations were also performed to calculate the energy of adsorption of C_3H_6 on the catalyst surface to understand the reaction pathways of C_3H_6 oxidation over CuO catalysts. Accordingly, a possible mechanism was proposed for catalytic oxidation of C_3H_6 over the CuO film catalyst using CJSR.

2. Experimental

2.1. Catalyst preparation

The CuO film catalysts were prepared using PSE-CVD and details can be found in our previous work [24]. During the deposition process, the dissolved $Cu(acac)_2$ precursor in a solvent of ethanol was injected into evaporation chamber kept at 200 °C then transported to the deposition chamber, where a flat resistive heating plate was used to heat the substrates to 325 °C. The experimental conditions of the CuO preparation are shown in Table S1 (Supplementary data).

2.2. Characterization

To reveal the relationship between the physio-chemical properties of the catalysts and their performances, several methods were involved for the analysis of the synthesized films. The crystalline structure was identified using X-ray diffraction (XRD) technique that performed under ambient conditions using Bruker D8 Focus equipped with a source of radiation of Cu Kα. The surface morphology was determined by Scanning Electron Microscope (SEM, S-4800 Hitachi) with ultra-high resolution of 1.5 nm (15 kV). The surface chemical composition was examined by the X-Ray photoelectron spectroscopy (XPS, ESCALAB 250Xi).

2.3. Catalytic test and kinetic study

C_3H_6 is encountered as exhaust emissions and difficult to be oxidized. Here, the catalytic activity of the CuO films was investigated via the deep oxidation of C_3H_6 at atmospheric pressure in a newly designed continuous CJSR. The design of CJSR can be seen in Figs. 1 and S1 (online) and more detailed information about it is described hereafter. It is made of fused silica to minimize induced catalytic reactions, consists of a small sphere of 50 mm inner diameter (~104 cm^3) and 4 nozzles with 0.3 mm inner diameter in the center of the reactor. The reactor is designed to be open and close based on the retention of the JSR four nozzle designs. In the selection of the middle connection mode, the use of ground glass interface with a snap connection was performed to ensure air tightness and take into account the reactor quartz glass material problems. In attempts to have sufficient pre-mixing space and docking space inside the reactor, the reactor sphere is elongated from the middle, thus a 20 mm long columnar structure is added to the middle of the two hemispheres. This part is a double-layer nested structure and grinding glass was used to ensure sealing. After testing, it can be secured that a maximum of 5.0 kPa pressure can be used to ensure the airtight that fully meet the requirements of the experimental tightness. Then to enable the reactor to be applied to a digital electric furnace for heating, the inlet and outlet pipes at both ends of the reactor are lengthened so that the reactor total length reaches 660 mm. In order to check the homogeneity of temperature, velocity magnitude and mole fractions of H_2O and CO_2 inside the reactor, we have performed some CFD modeling calculations using ANSYS Fluent software and detailed information about the setting parameters are listed in Table 1.

During the experiments, a gas mixture consisted of 0.5%–1.5% C_3H_6 and 5%–40% O_2 in a flow of Ar was introduced continuously into the reactor, with the gaseous hourly space velocity (GHSV) of 70,000 mL g_{cat}^{-1} h^{-1}. The residence time inside the flow CJSR varies with the reaction temperature, and the value reaches second scale within the range of 1.12–7.84 s. The furnace temperature was raised with a ramp of 2 °C min^{-1}. A K-type thermocouple located at an isolated quartz tube in the center of the CJSR was used to measure the temperature during the experiments. The outlet gases were analyzed by GC (Agilent GC3000) for qualitative and quantitative analysis, equipped with the capillary columns (Al_2O_3-KCl, Molecular Sieve-5A, and HP-INNOWax), the thermal conductivity detector (TCD), and the flame ionization detector (FID). The experimental errors estimated for mole fractions are within ±5%.

2.4. Theoretical calculation

The C_3H_6 adsorption and reaction behaviors on CuO surface were studied by using DFT calculation. The generalized gradient approximation (GGA) with Perdew-Burke-Ernzerhof (PBE) functional was applied for the exchange and correlation potentials [27]. According to the preferred orientation plane exhibited by XRD analysis, perfect CuO (1 1 1) surface model was established to investigate the CuO surface properties with p(3 × 2) surface expansion. The surface slab comprised of three Cu atomic layers and three O atomic layers. A sheet of 12 Å vacuum layer was placed above the surface plane to avoid interference from imaging surfaces. Possible adsorbed oxygen structure on the CuO (1 1 1) surface was found and its activity in reacting with C_3H_6 in comparison with lattice oxygen was studied.

3. Results and discussion

3.1. Structure

XRD analysis was performed in attempts to exhibit the crystalline structure of the thin films deposited at 325 °C and the XRD patterns are presented in Fig. 2. The diffraction peaks are observed at 2θ of 32.74°, 35.57°, 38.75°, 49.01°, 61.64°, 66.05° and 68.26°, corresponding to (1 1 0), (1 1 −1), (1 1 1), (2 0 −2), (1 1 −3), (3 1 −1) and (2 2 0) orientations of CuO. All the diffracted peaks fit well with the monoclinic of CuO structure (JCPDS No. 48–1548) and no peaks of impurity phases were shown, which reveals a high purity of the all deposited films.

The crystalline size and micro-strain of the film were estimated to be ~ 51 nm and 0.10%, respectively. The size here is slightly smaller when comparing to that of CuO catalyst in Ref. [22] (58 nm). It was also reported that the catalytic activity is generally higher with smaller particle size [24]. Furthermore, the small grain size is commonly known to have a beneficial effect on active sites dispersion, which is necessary to improve the catalytic activity

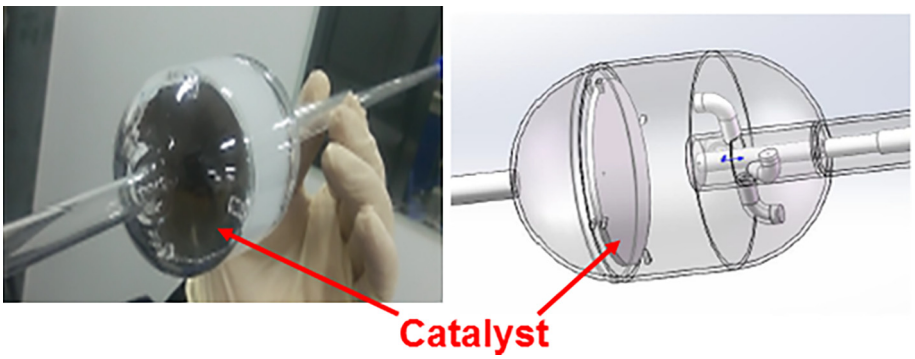

Fig. 1. (Color online) Catalytic jet-stirred reactor (CJSR).

Table 1
Boundary conditions and main simulation parameters.

Parameter	Value
Inlet boundary	Velocity-inlet, T = 800 K, P = 1 atm ($1\ atm = 1.013 \times 10^5\ Pa$), V = 7.04 m s^{-1}, turbulence intensity = 10%, hydraulic diameter = 1 mm
Outlet boundary	Pressure-outlet, T = 400 K, P = 1 atm, turbulence intensity = 10%, hydraulic diameter = 4 mm
Wall boundary	No slip conditions, T = 800 K

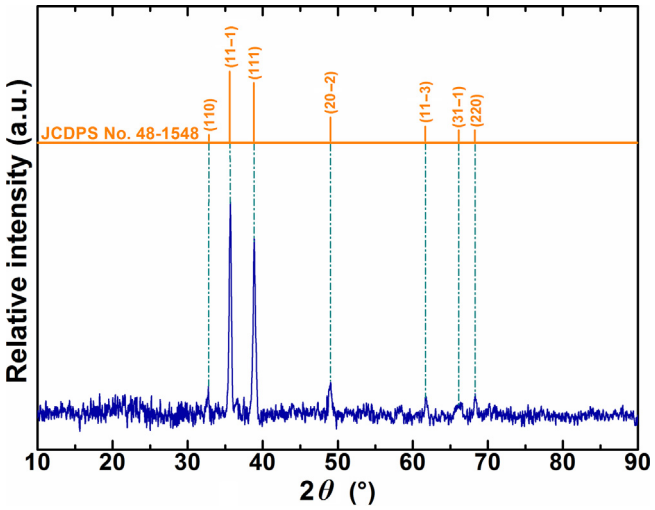

Fig. 2. (Color online) XRD pattern of the CuO thin film deposited on glass.

[28]. In this regard, the results obtained here could further benefit for the catalytic reaction.

3.2. Morphology

The surface morphology of the catalyst film was analyzed using SEM, as shown in Figs. 3 and S2 (online). It can be seen that the deposited film is morphologically homogeneous, uniform and continuous. The prepared film presents an open and porous texture and consists of nano-sized cubic embedded grains in a matrix that are comparable to the size determined from XRD results. The observed morphology with small grain size and open porosity is expected to offer high specific surface area, which could hold an important amount of oxygen and provide more accessible active catalytic sites that could be beneficial to the catalytic oxidation of VOCs.

3.3. Chemical composition

The surface chemical compositions and oxidation states of the films were analyzed using XPS. Fig. 4 shows the high-resolution XPS of Cu 2p and O 1s, and the entire spectra of the deposited films at the surface and in the bulk are presented in Fig. S3 (online). The spectrum of Cu 2p shows the presence of two major peaks of Cu $2p_{3/2}$ and Cu $2p_{1/2}$ located at binding energies (BE) of 933.5 and 953.3 eV, respectively, that are in line with previously reported results [29]. The O 1 s spectrum was deconvoluted into two main components in the BE range of 529–532 eV as presented in Fig. 4b. The peak located at 529.51 eV is characteristic of the lattice oxygen (O_{Lat}) species O^{2-}, while the peak at higher binding energy (~531.73 eV) is attributed to the presence of adsorbed oxygen (O_{Ads}) species [29,30]. The atomic ratio of O/Cu at the surface revealed a high content of oxygen in the deposited films, which confirms that the high amount of oxygen is presented in the open morphology structure of the films.

After 28.5 nm etching, the content of the chemical elements changed from the non-etched one as shown in Table 2 and Fig. 4c. The obtained atomic ratio of O and Cu at the surface of the deposited films is ~1 after etching. The latter is in line with the XRD result and confirms the purity of the CuO crystalline structure. For total oxygen (O_{tot}), even its atomic content increased in the films after etching, O_{Ads} content was significantly decreased. This variation in O_{Ads}, from the surface to the bulk, is accompanied by a slight shift in its XPS peak from 531.73 to lower binding energy value of 531.02 eV, as shown from Fig. 4b and c. In addition, in line with the variations of O_{Ads} content, the peak attributed to C 1 s that mainly comes from the ambient air or the decomposition of the precursor, decreased significantly to quite negligible value in the bulk. The latter confirms that the C1s is almost adsorbed on the surface but not incorporated in the structure of CuO films. Hence, the observed shift of O_{Ads} peak into lower BE value can be explained by the significant decrease in C1s that was bonded to O_{Ads} at CuO surface, thus likewise the BE of O_{Ads} decreases to lower value. Furthermore, the fitted profiles, after etching, of O_{Lat} and O_{Ads} were found to agree well with the measured profiles, as shown in Fig. 4. Thus, the observed high oxygen content at the surface and the negligible amount of carbon impurity in the deposited films are expected to enhance the catalytic behavior with respect to complete abatement of exhaust gases.

3.4. Catalytic performance

The catalytic performance of the CuO films coated on mesh of stainless steel was performed for complete oxidation of C_3H_6 at atmospheric pressure using CJSR. Considering the effect of non-coated mesh, the tests were also carried out over non-coated mesh

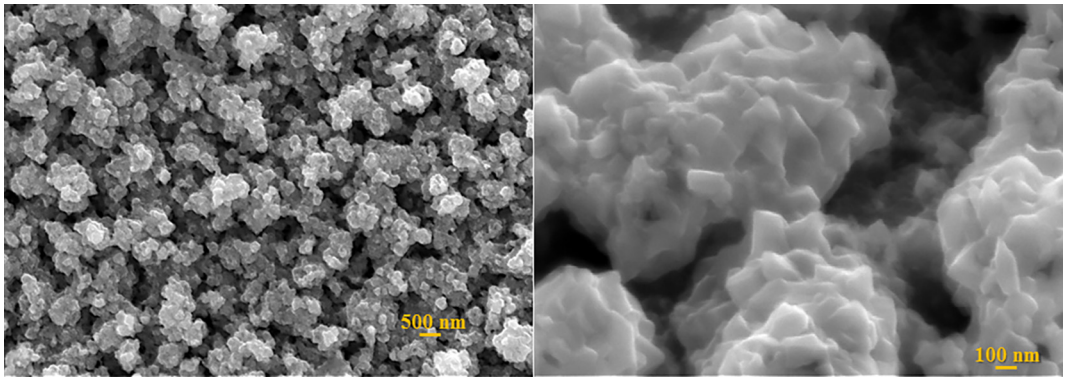

Fig. 3. (Color online) SEM images of deposited CuO samples supported on grid mesh.

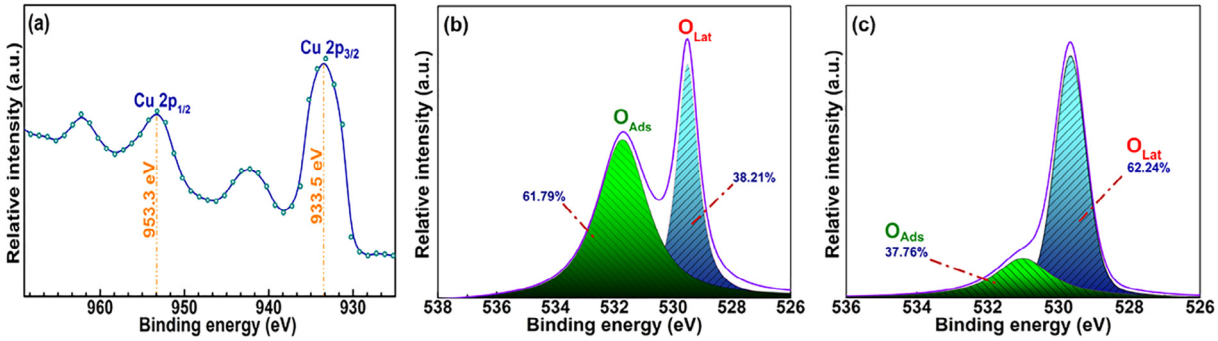

Fig. 4. (Color online) XPS spectra of (a) Cu 2p, and (b, c) O 1s before and after etching.

Table 2
Surface composition of CuO thin films before and after etching.

Elements	Before etching	After etching
Cu (At%)	26.4	46.5
O_{tot} (At%)	59.3	52.4
O/Cu	2.6	1.1
C (At%)	14.4	1.1
O_{Ads}/O_{tot} (At%)	61.8	37.8

under the same experimental conditions and with an oxygen concentration of 10% in the gas mixture. In attempts to investigate the effect of oxygen concentration on the catalytic oxidation of C_3H_6, different concentrations of oxygen (5%, 10%, 20%, 30% and 40%) were used in the gas mixture. Fig. 5 shows the conversion-temperature profiles (known as light-off curves) of C_3H_6 to CO_2 over CuO catalysts. The results showed that CuO-coated mesh permits to shift total oxidation temperatures towards much lower values when comparing to non-coated mesh. The onset of C_3H_6 conversion occurs almost at 200 °C and the total conversion takes place at 430 °C over CuO, while at the latter value, the conversion was just achieved 21% conversion on the non-coated mesh. The reproducibility of the obtained results was evaluated by reusing the CuO catalyst several times and very good results were obtained, as shown in Figs. 6 and 7. It should be noted that using CuO catalyst, no trace of CO was detected during the oxidation process, which reflects that CuO is a very active catalyst for complete C_3H_6 oxidation. However, with non-coated mesh, a certain amount of CO was detected. These results demonstrate that CJSR is an efficient and clean catalytic reactor for deep oxidation of C_3H_6 at low temperature. In addition, the CFD calculation showed very good homogeneity of the flow inside the reactor in terms of temperature, velocity magnitude and mole fractions as shown in Fig. 8.

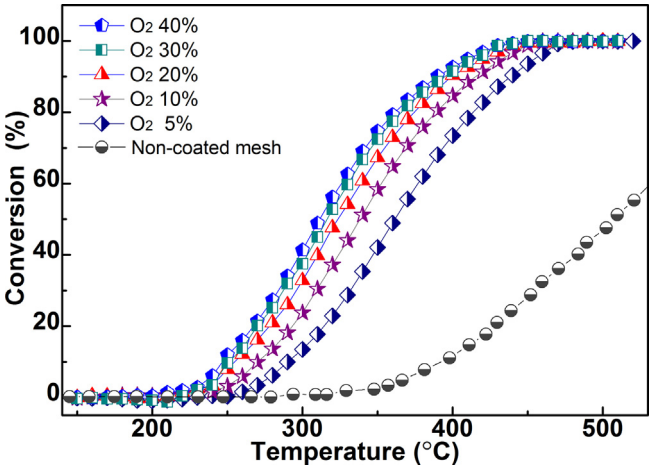

Fig. 5. (Color online) Conversion-temperature curves of C_3H_6 over CuO-coated mesh of stainless steel and non-coated mesh.

Moreover, as can be seen from Fig. 5, the conversion temperature values of T_{10}, T_{50} and T_{90} (correspond to 10%, 50% and 90% C_3H_6 conversion, respectively) decrease gradually with the increase of oxygen concentration, which means the oxygen content promotes the reactivity and reduces the consumption energy during the reaction. In comparison to the catalytic C_3H_6 oxidation behavior for a number of interesting catalysts such as noble supported on Al_2O_3 ($T_{90} \sim 412$ °C) [31,32] and/or non-noble metal oxides as Mn_3O_4 and $Co_{1.02}Mn_{1.98}O_4$ ($T_{90} \sim 520$ °C) [33] that usually performed in flow reactor, the catalytic performance of CJSR using CuO catalyst exhibits quite promising catalytic performance with a value of T_{90} of ~375 °C.

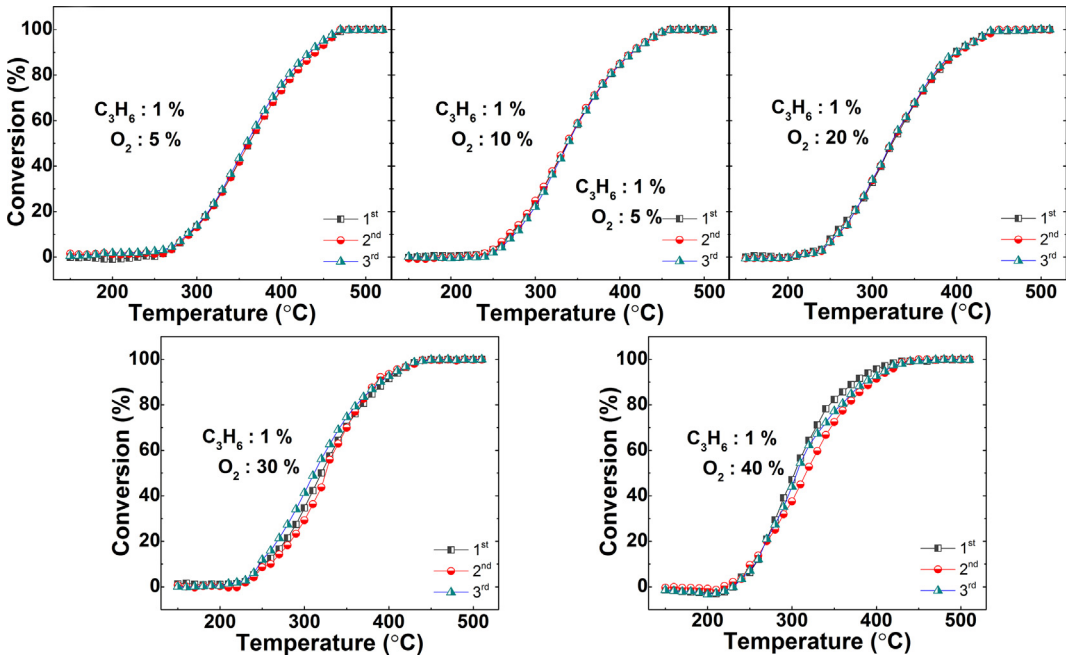

Fig. 6. (Color online) Reproducibility of C_3H_6 conversion over CuO-coated mesh of stainless steel, using different O_2 concentrations.

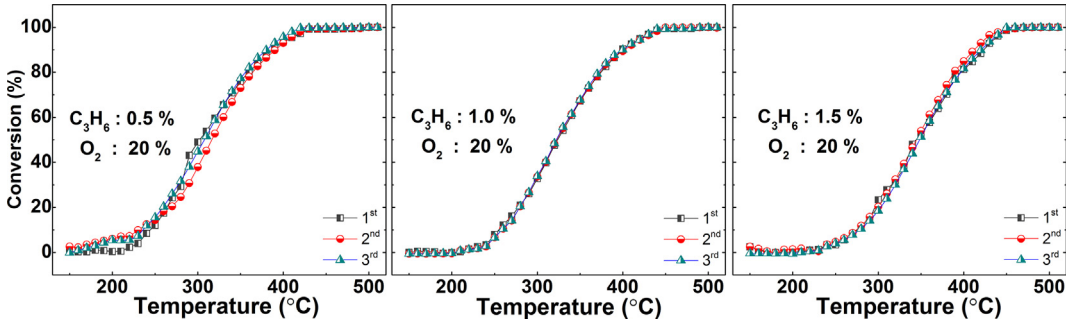

Fig. 7. (Color online) Reproducibility of C_3H_6 conversion over CuO-coated mesh of stainless steel, using different C_3H_6 concentrations.

Also, a comparison of the catalytic performance was made based on the specific reaction rate [34], as well as the apparent activation energies (E_{appa}) determined by Arrhenius equation based on the light-off curves where C_3H_6 conversion is less than 15%. The reaction rate of propene removal was calculated from the molar flow rate (F_0) and the conversion (X) achieved at 320 °C then normalized to the specific surface area using the following equation

$$r = F_0 X_{(320\ ^\circ C)}/S_{BET}\left(\mu mol\ m^{-2}h^{-1}\right), \quad (1)$$

where F_0 is the molar flow rate, X the conversion achieved at 320 °C and S_{BET} the specific surface area.

As displayed in Fig. 9, the reaction at 5% concentration oxygen exhibits the lowest rate of C_3H_6 conversion (13.64 μmol m^{-2} h^{-1}), whereas increasing oxygen concentration up to 30% enhances the latter rate by more than a factor of two. This incensement in reaction rate is in line with the previously observed enhancement in catalytic activity when increasing oxygen content in the flow, reflecting that oxygen is strongly involved in the reaction and has a significant effect on the catalytic performance. However, over 30% oxygen concentration, the reaction rate is still comparable to the rate measured for 40% oxygen concentration, and the catalytic conversions for these cases remained quite similar. Thus, such phenomenon indicates that the oxygen concentration has been close to oxygen demand for complete conversion of C_3H_6 over CuO catalyst.

In attempts to understand the process change in reaction rate at different temperatures during the catalytic oxidation of C_3H_6 on CuO catalyst, the variation of reaction rate with temperature was calculated and plotted, as shown in Fig. 10. It can be seen during the entire catalytic reaction that at the initial reaction temperature of 200 °C, the catalytic oxidation was not started where the reaction rate was zero. As the temperature gradually increased, the conversion of C_3H_6 started and accompanied by an increase in the reaction rate. Since the latter is a proportional parameter to the conversion, the law of the reaction rate is related to the conversion temperature. By increasing the reaction temperature, the reaction rate is getting increased and more energy barriers for the oxidation of C_3H_6 molecules become satisfied. Considering the oxygen concentration to be in excess, the effect of C_3H_6 concentration can be investigated and the reaction rate expression can be simplified to a power law equation as follows:

$$r = k \cdot [C_3H_6]^n, \quad (2)$$

where k, $[C_3H_6]$ and n represent the kinetic rate constant, C_3H_6 concentration and reaction order, respectively. The values of kinetic rate constant and reaction order were obtained from the plot of reaction rate against $[C_3H_6]$ (at 320 °C), then fitted using the above

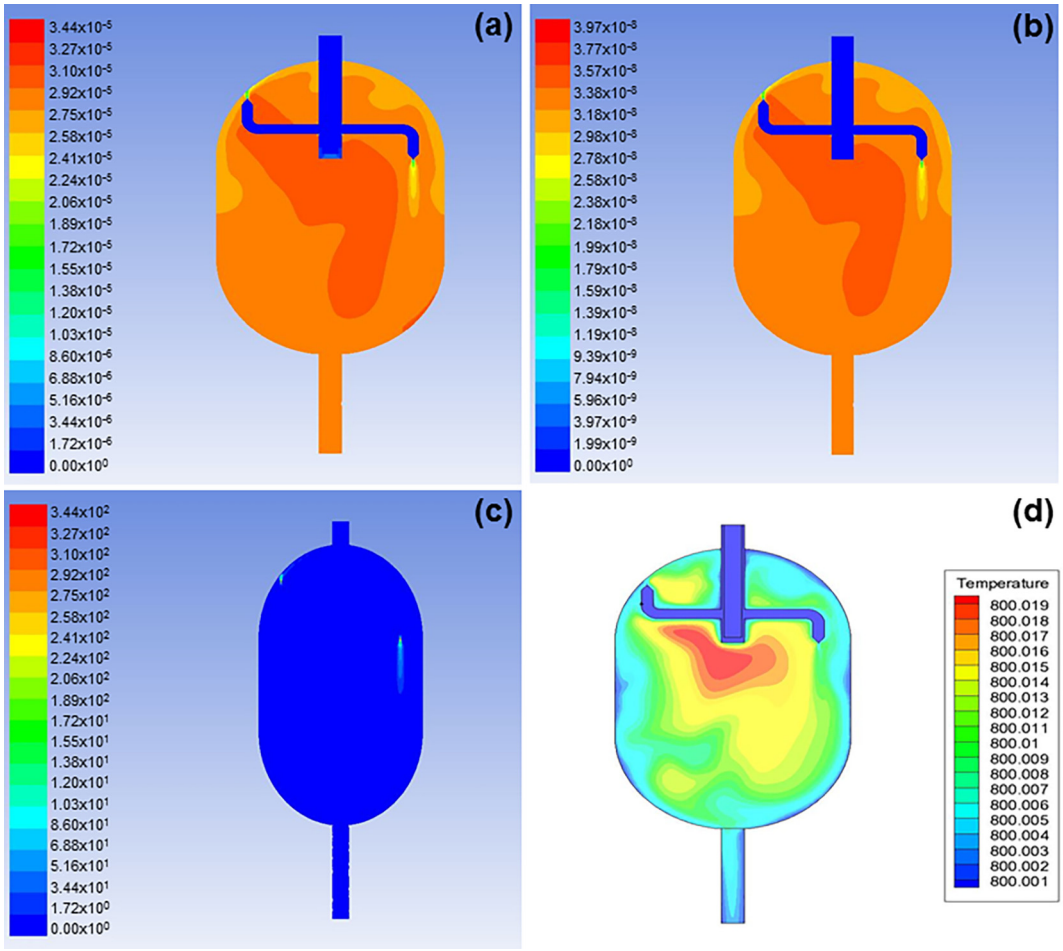

Fig. 8. (Color online) CFD calculation showed very good homogeneity of the flow inside the reactor in terms of (a, b) mole fractions, (c) velocity magnitude and (d) temperature.

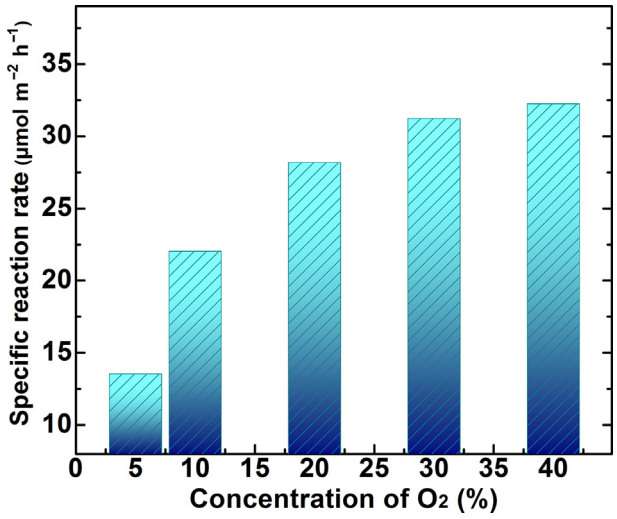

Fig. 9. (Color online) Specific reaction rate of C_3H_6 oxidation at 320 °C with different concentration of O_2.

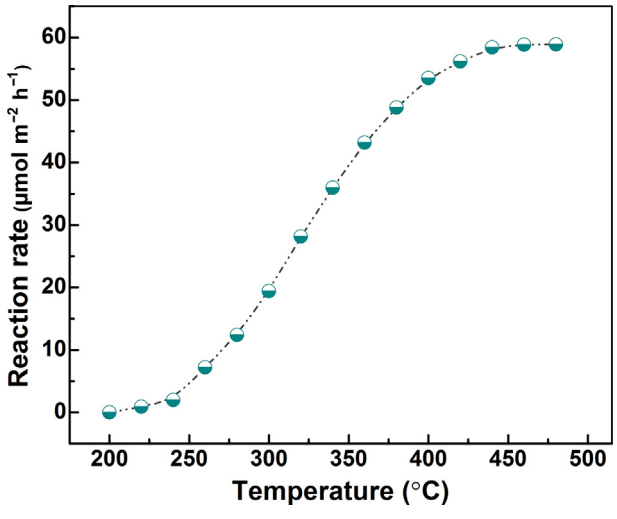

Fig. 10. (Color online) Variation of the reaction rate of C_3H_6 as function of reaction temperature.

power law equation as shown in Fig. 11. The fitting coefficient value of R^2 was around 0.96, indicating that the experimental results were well represented by the power law model. The decrease in reaction rate of [C_3H_6] incensement can be explained by the high [C_3H_6] with the limitation of active sites capacity on the surface of the catalyst.

Furthermore, the difference in light-off curves behavior may also be linked to the difference observed in E_{appa}, as shown in Fig. 12. The higher E_{appa} is, the lower conversion temperature of C_3H_6, is in good agreement with Refs. [22,35]. It is also observed that the increase in catalytic performance with increasing the

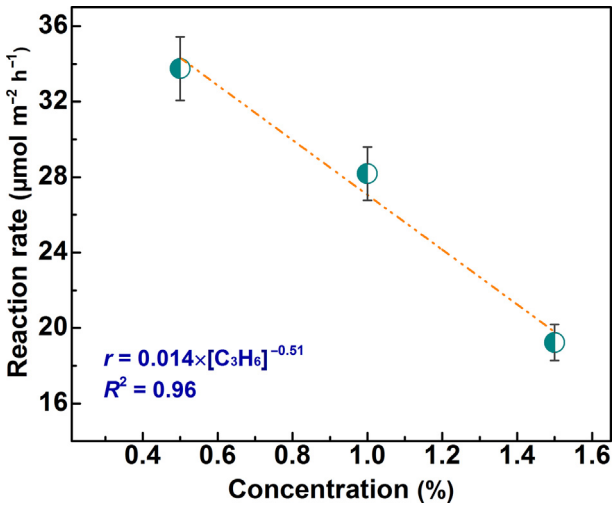

Fig. 11. (Color online) C_3H_6 reaction rate over CuO catalyst fitted with power law equation, calculated at 320 °C.

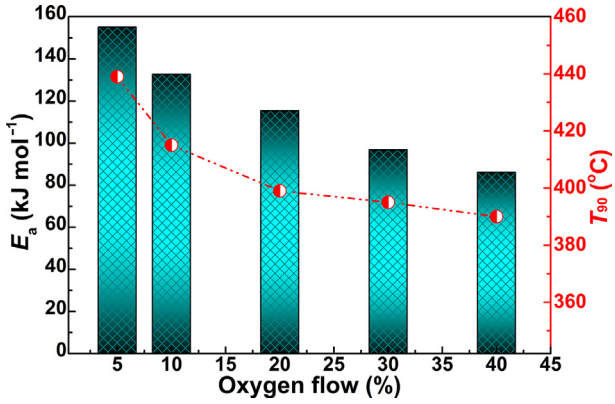

Fig. 12. (Color online) Apparent activation energy and T_{90} for catalytic oxidation C_3H_6, calculated from data where conversion is less than 15%.

oxygen concentration is accompanied by decreasing in E_{appa}. Moreover, compared to other catalysts that present higher activation energies E_{appa} [35,36], the used CuO catalyst with CJSR exhibited a very good catalytic performance in terms of activity.

It has been commonly accepted that the catalytic oxidation of hydrocarbons on transition metal oxide catalysts can follow the Mars-van Krevelen (MvK) mechanism [37], in which the C-H bond activation is related to the oxidation rate of hydrocarbons. According to the SEM results, the open porosity can engender many accessible active sites as well as provide pre-disposed space holding a great amount of oxygen that has been also confirmed by XPS results. The catalytic oxidation of C_3H_6 over CuO is assumed to involve alternate reduction and oxidation of the oxides with the formation of surface oxygen vacancies and their replenishment by the adsorption and dissociation of oxygen gas phase [38,39]. Hence, the previous explanations demonstrate that the open porosity texture of CuO deposit films plays an important role in the C_3H_6 oxidation process, which is in good correlation with Ref. [22]. As a consequence, the application of a simple synthesized CuO catalyst, with these good properties, using CJSR could provide very good catalytic performance in terms of activity and could further pave the way for other catalytic reactions at low temperature.

Furthermore, to better understand the C_3H_6 adsorption and reaction behaviors on CuO film surface, the theoretical calculation was performed using the DFT method. The adsorption energy values of C_3H_6 on O_{Ads} and O_{Lat} of CuO surface were found to be –1.805 and 0.258 eV (Fig. 13), respectively. These values demonstrate that the reaction pathway on O_{Ads} is more likely plausible than on O_{Lat}. Moreover, the partial density of states (PDOS) and density of states (DOS) analyses of C_3H_6 on O_{Ads} and O_{Lat} of the CuO surface, as presented in Fig. 14, showed that the p orbital of O_{Ads} and O_{Lat} are the important contributors to surface activity. These findings reflect that the O_{Ads} is the most possible involved oxygen during the catalytic reaction of C_3H_6 on CuO thin catalyst, which is in good accordance with the aforementioned experimental results. Furthermore, although the reaction energy profile of propene with lattice oxygen has been reported previously [40], but the reaction energy profile of propene with adsorbed O over the CuO surface is still not well understood to the best of our knowledge. The energy profile of C_3H_6 reaction with adsorbed O is shown in Fig. 15. The Eley-Rideal type surface reaction path was studied considering three kinds of propene oxidation products including adsorbed OH and gaseous propenyl, adsorbed OH and adsorbed propenyl, and propene oxide. The results showed that the production of propenyl needs to overcome the energy barriers of 4.493 and 4.046 eV, respectively. In comparison, the production of propene oxide only needs to overcome an energy barrier of 0.948 eV, which makes this reaction more likely to proceed. Finally, the ability of newly-designed catalytic jet-stirred reactor (CJSR) to

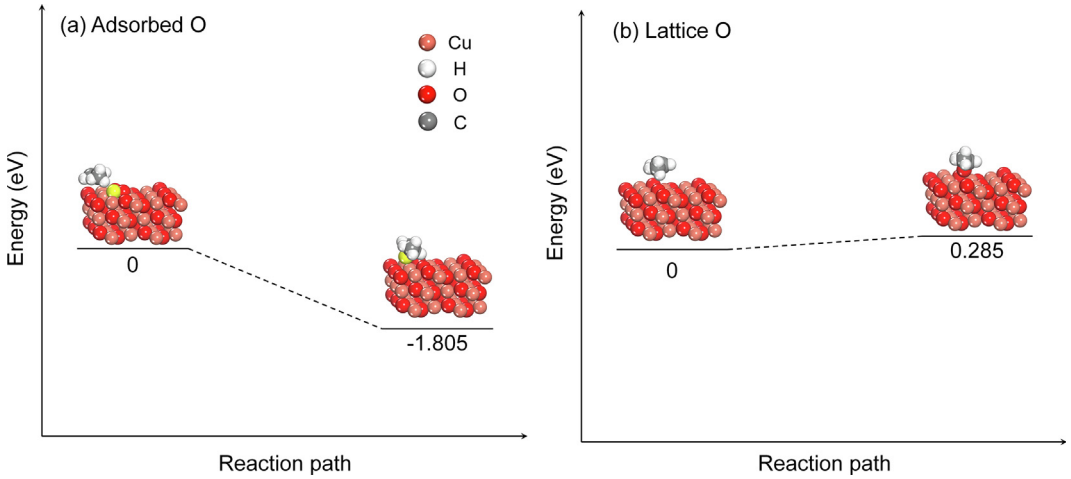

Fig. 13. (Color online) Energy profiles of C_3H_6 reaction. (a) Adsorbed O and (b) Lattice O of CuO surface.

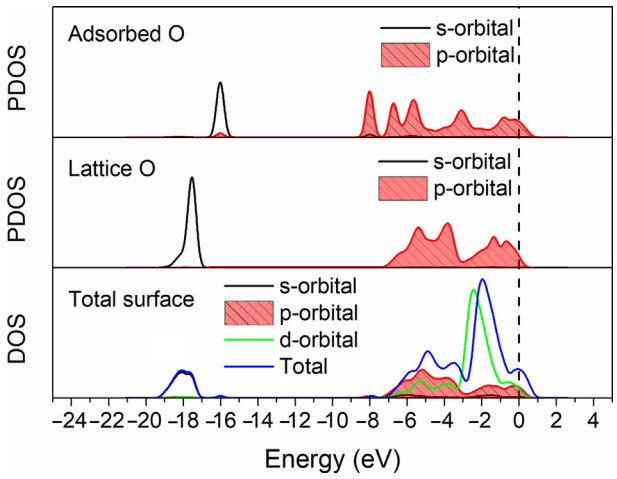

Fig. 14. (Color online) DOS analysis of C_3H_6 adsorption on CuO surface.

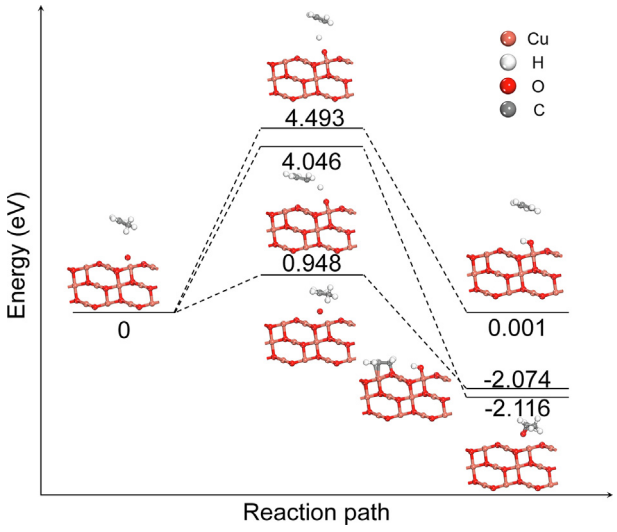

Fig. 15. (Color online) The energy profile of C_3H_6 reaction with adsorbed O over the CuO surface.

perform a kinetic study of the C_3H_6 catalytic oxidation over CuO thin catalyst has been proved, which was attributed to the high residence time provided by CJSR allowing enough contact time of C_3H_6 and active oxygen surface of CuO catalyst.

4. Conclusions

The novel catalytic jet-stirred reactor was successfully investigated for the heterogeneous kinetic study of the complete oxidation of propene in presence of CuO thin film catalysts at low temperature. The deposited film catalysts exhibited the pure crystalline structure of CuO with nano-sized crystallite of 51 nm, and open and porous structure that can hold an important amount of adsorbed oxygen as exhibited by surface composition analysis using XPS technique. Furthermore, the catalytic tests using CJSR indicate that CuO film catalyst is very active for the complete oxidation of propene, with a performance comparable to those of supported noble metals. The relationship between the catalyst properties and the catalytic performance of CJSR has been revealed. The kinetic study revealed an incensement in reaction rate with increasing oxygen content in the flow owing to the high residence time offered by CJSR; while above 30% of O_2 the reaction rate increases slightly which is attributed to the catalyst surface saturation. The correlation between reaction rate and activation energy with the catalytic performance within the novel reactor design was established. Furthermore, theoretical calculations using DFT method demonstrated that O_{Ads} is the most involved oxygen in the catalytic reaction of C_3H_6 over CuO surface catalyst. Thus, the newly-designed catalytic jet-stirred reactor could provide a good efficient mixing and thermal control that could result in obtaining a high product yield and selectivity; this advantage could open the doorway for other gaseous molecules to improve their catalytic oxidation performance owing to the long residence time and enough contact time of gas-catalyst surface, and also perform kinetic study with high residence time at low temperature.

Conflict of interest

The authors declare that they have no conflict of interest.

Acknowledgments

The authors thank the financial support from the Ministry of Science and Technology of China (2017YFA0402800), the National Natural Science Foundation of China (51476168 and 91541102) and Recruitment Program of Global Youth Experts. Dr. El Kasmi is so grateful to the support of Chinese Academy of Sciences for senior international scientists within the framework of PIFI program (2017PE0009). CFD modeling of the CJSR reactor by Mr. Chao-Jie Song and Prof. Zun-Hua Zhang is also acknowledged.

Author contributions

Achraf El Kasmi treated the data and wrote the article; Guan-Fu Pan carried out experimental work and treated the data; Ling-Nan Wu took care of calculation part; Zhen-Yu Tian designed the experiments and revised the article.

Appendix A. Supplementary data

Supplementary data to this article can be found online at https://doi.org/10.1016/j.scib.2019.04.001.

References

[1] Mi Z, Zheng J, Meng J, et al. Carbon emissions of cities from a consumption-based perspective. Appl Energy 2019;235:509–18.
[2] Zhou T, Ren L, Liu H, et al. Impact of 1.5 °C and 2.0 °C global warming on aircraft takeoff performance in China. Sci Bull 2018;63:700–7.
[3] Wang C, Bi J, Olde Rikkert MGM. Early warning signals for critical transitions in cardiopulmonary health, related to air pollution in an urban Chinese population. Environ Int 2018;121:240–9.
[4] Wang X, Jiang D, Lang X. Future extreme climate changes linked to global warming intensity. Sci Bull 2017;62:1673–80.
[5] Dauchet L, Hulo S, Cherot-Kornobis N, et al. Short-term exposure to air pollution: associations with lung function and inflammatory markers in non-smoking, healthy adults. Environ Int 2018;121:610–9.
[6] Paulsen AD, Kunsa TA, Carpenter AL, et al. Gaseous and particulate emissions from a chimneyless biomass cookstove equipped with a potassium catalyst. Appl Energy 2019;235:369–78.
[7] Wang X, Huang K, Qian J, et al. Enhanced CO catalytic oxidation by Sr reconstruction on the surface of $La_xSr_{1-x}CoO_{3-\delta}$. Sci Bull 2017;62:658–64.
[8] Guo Z, Liu B, Zhang Q, et al. Recent advances in heterogeneous selective oxidation catalysis for sustainable chemistry. Chem Soc Rev 2014;43:3480–524.
[9] Fan S-B, Kouotou PM, Weng J-J, et al. Investigation on the structure stability and catalytic activity of Cu–Co binary oxides. Proc Combust Inst 2017;36:4375–82.
[10] Huang H, Xu Y, Feng Q, et al. Low temperature catalytic oxidation of volatile organic compounds: a review. Catal Sci Technol 2015;5:2649–69.
[11] Tian Z-Y, Mountapmbeme Kouotou P, El Kasmi A, et al. Low-temperature deep oxidation of olefins and DME over cobalt ferrite. Proc Combust Inst 2015;35:2207–14.

[12] Zhang Z, Jiang Z, Shangguan W. Low-temperature catalysis for VOCs removal in technology and application: a state-of-the-art review. Catal Today 2016;264:270–8.
[13] Herbinet O, Dayma G. Jet-stirred reactors. Clean. Combust.. Springer, London; 2013. p. 183–210.
[14] Wittstock A, Zielasek V, Biener J, et al. Nanoporous gold catalysts for selective gas-phase oxidative coupling of methanol at low temperature. Science 2010;327:319–22.
[15] Nodehi Z, Rafati AA, Ghaffarinejad A. Palladium-silver polyaniline composite as an efficient catalyst for ethanol oxidation. Appl Catal Gen 2018;554:24–34.
[16] Tian M, He C, Yu Y, et al. Catalytic oxidation of 1,2-dichloroethane over three-dimensional ordered meso-macroporous $Co_3O_4/La_{0.7}Sr_{0.3}Fe_{0.5}Co_{0.5}O_3$: destruction route and mechanism. Appl Catal Gen 2018;553:1–14.
[17] Li WB, Wang JX, Gong H. Catalytic combustion of VOCs on non-noble metal catalysts. Catal Today 2009;148:81–7.
[18] Kan J, Deng L, Li B, et al. Performance of Co-doped Mn-Ce catalysts supported on cordierite for low concentration chlorobenzene oxidation. Appl Catal Gen 2016;530:21–9.
[19] Xie X, Li Y, Liu Z-Q, et al. Low-temperature oxidation of CO catalysed by Co_3O_4 nanorods. Nature 2009;458:746–9.
[20] Wang L, Gong H, Wang C, et al. Facile synthesis of novel tunable highly porous CuO nanorods for high rate lithium battery anodes with realized long cycle life and high reversible capacity. Nanoscale 2012;4:6850–5.
[21] Zhou N, Yuan M, Li D, et al. One-pot fast synthesis of leaf-like CuO nanostructures and CuO/Ag microspheres with photocatalytic application. Nano 2017;12:1750035.
[22] Tian ZY, Herrenbrück HJ, Kouotou PM, et al. Facile synthesis of catalytically active copper oxide from pulsed-spray evaporation CVD. Surf Coat Technol 2013;230:33–8.
[23] Chen MS, Goodman DW. The structure of catalytically active gold on Titania. Science 2004;306:252–5.
[24] El Kasmi A, Tian Z-Y, Vieker H, et al. Innovative CVD synthesis of Cu_2O catalysts for CO oxidation. Appl Catal B Environ 2016;186:10–8.
[25] Tian Z-Y, Mountapmbeme Kouotou P, Bahlawane N, et al. Synthesis of the catalytically active Mn_3O_4 spinel and its thermal properties. J Phys Chem C 2013;117:6218–24.
[26] Tchoua NPH, El Kasmi A, Weiss T, et al. Investigation of the growth behaviour of cobalt thin films from chemical vapour deposition, using directly coupled X-ray photoelectron spectroscopy. Z Für Phys Chem 2015;229:1887–905.
[27] Perdew JP, Burke K, Ernzerhof M. Generalized gradient approximation made simple. Phys Rev Lett 1996;77:3865–8.
[28] Qadir K, Joo SH, Mun BS, et al. Intrinsic relation between catalytic activity of CO oxidation on Ru nanoparticles and Ru oxides uncovered with ambient pressure XPS. Nano Lett 2012;12:5761–8.
[29] Biesinger MC, Lau LWM, Gerson AR, et al. Resolving surface chemical states in XPS analysis of first row transition metals, oxides and hydroxides: Sc, Ti, V, Cu and Zn. Appl Surf Sci 2010;257:887–98.
[30] Powell CJ, Jablonski A. NIST electron effective-attenuation-length database - version 1.3. National Institute of Standards and Technology, Gaithersburg, 2011
[31] Ivanova S, Petit C, Pitchon V. Application of heterogeneous gold catalysis with increased durability: oxidation of CO and hydrocarbons at low temperature. Gold Bull 2006;39:3–8.
[32] Gluhoi AC, Bogdanchikova N, Nieuwenhuys BE. The effect of different types of additives on the catalytic activity of Au/Al_2O_3 in propene total oxidation: transition metal oxides and ceria. J Catal 2005;229:154–62.
[33] Tian ZY, Bahlawane N, Vannier V, et al. Structure sensitivity of propene oxidation over Co-Mn spinels. Proc Combust Inst 2013;34:2261–8.
[34] Liotta LF, Ousmane M, Di Carlo G, et al. Total oxidation of propene at low temperature over Co_3O_4–CeO_2 mixed oxides: Role of surface oxygen vacancies and bulk oxygen mobility in the catalytic activity. Appl Catal Gen 2008;347:81–8.
[35] Pan G-F, Fan S-B, Liang J, et al. CVD synthesis of Cu_2O films for catalytic application. RSC Adv 2015;5:42477–81.
[36] Liang J, Pan G-F, Fan S-B, et al. CVD synthesis and catalytic combustion application of chromium oxide films: CVD synthesis and catalytic combustion application of chromium oxide films. Phys Status Solidi C 2015;12:1001–5.
[37] Doornkamp C, Ponec V. The universal character of the Mars and Van Krevelen mechanism. J Mol Catal Chem 2000;162:19–32.
[38] Bao H, Chen X, Fang J, et al. Structure-activity relation of Fe_2O_3-CeO_2 composite catalysts in CO oxidation. Catal Lett 2008;125:160–7.
[39] Aneggi E, Llorca J, Boaro M, et al. Surface-structure sensitivity of CO oxidation over polycrystalline ceria powders. J Catal 2005;234:88–95.
[40] Song Y-Y, Wang G-C. A DFT study and microkinetic simulation of propylene partial oxidation on CuO (111) and CuO (100) surfaces. J Phys Chem C 2016;120:27430–42.

Achraf El Kasmi received his Ph.D. degree in chemical engineering and materials science from University of Abdelmalek Essaadi in July 2016. During his doctoral study, he spent 2 years at the University of Bielefeld in Germany as a DAAD scholar. He is currently a post-doctoral fellow researcher at Institute of Engineering Thermophysics, Chinese Academy of Sciences (CAS). His current research interests include thin film materials and their applications in environment and energy.

Zhen-Yu Tian received his Ph.D. degree from University of Science and Technology of China in 2008. He then worked as postdoctoral at CNRS of Nancy till 2010, and served as Humboldt scholar and team leader at the University of Bielefeld from 2010 to 2013. In 2013, he joined the Institute of Engineering Thermophysics, CAS, as a Full Professor. His current research interests are combustion kinetics, low temperature oxidation, and catalytic combustion.